The carboxyl-terminal extension on fungal mitochondrial DNA polymerases: Identification of a critical region of the enzymefrom Saccharomyces cerevisiae

ARTICLE *in* YEAST · JANUARY 2006

Impact Factor: 1.63 · DOI: 10.1002/yea.1344 · Source: PubMed

Yeast
Yeast 2006; **23**: 101–116.
Published online in Wiley InterScience (www.interscience.wiley.com). **DOI:** 10.1002/yea.1344

Research Article

The carboxyl-terminal extension on fungal mitochondrial DNA polymerases: identification of a critical region of the enzyme from *Saccharomyces cerevisiae*

Matthew J. Young, Steven S. Theriault[#], Mingyi Li and Deborah A. Court*
Department of Microbiology, University of Manitoba, Winnipeg, MB, Canada R3T 2N2

**Correspondence to: Deborah A. Court, Department of Microbiology, 301 Buller Building, University of Manitoba, Winnipeg, Canada MB R3T 2N2.*
E-mail: Deborah_Court@UManitoba.ca

[#]Present address: Department of Medical Microbiology, University of Manitoba, Winnipeg, MB, Canada R3T 2N2.

Received: 16 July 2005
Accepted: 5 December 2005

Abstract

Fungal mitochondrial DNA (mtDNA) polymerases, in comparison to their metazoan counterparts, harbour unique carboxyl-terminal extensions (CTEs) of varying lengths and unknown function. To determine the essential regions of the 279 residue CTE of the yeast enzyme (Mip1p), several CTE-truncation variants were expressed in *Saccharomyces cerevisiae*. The respiratory competence of *mip1Δ175* cells, in which Mip1p lacks the C-terminal 175 residues, is indistinguishable from that of wild-type. In contrast, strains harbouring Mip1pΔ351 and Mip1pΔ279 rapidly lose mtDNA. Approximately one in six *mip1Δ216* transformants grew on glycerol, albeit poorly. Fluorescence microscopy and Southern blot analysis revealed lower levels of mtDNA in these cells, and the rapid loss of mtDNA during fermentative, but not respiratory, growth. Therefore, only the polymerase-proximal segment of the Mip1p CTE is necessary for mitochondrial function. Comparison of this essential segment with the sequences of other fungal mtDNA polymerases revealed novel features shared among the mtDNA polymerases of the Saccharomycetales. Copyright © 2006 John Wiley & Sons, Ltd.

Keywords: mitochondrial DNA polymerase; *Saccharomyces*; mitochondrial DNA maintenance; erythromycin-resistance; respiration; fungi; phylogeny

Introduction

Mitochondria are the sites of oxidative phosphorylation in eukaryotic cells. These organelles harbour mitochondrial genomes or mitochondrial DNAs (mtDNAs) that encode subunits of the respiratory chain, rRNAs, tRNAs and, in some cases, ribosomal proteins. In obligately aerobic organisms, such as humans, base-substitution, deletion and duplication mutations in mtDNA result in a variety of degenerative diseases. These mutations most likely result from errors in mtDNA replication (reviewed by Kaguni, 2004).

The ascomycetous fungus *Saccharomyces cerevisiae* has been used extensively for studies of mtDNA replication, due in part to its ability to bypass the need for respiration in the presence of fermentable carbon sources. Haploid yeast cells typically contain 40–50 copies (Grimes *et al*., 1974) of an 86 kb mtDNA with a circular genetic map (Foury *et al*., 1998). Studies of mtDNA replication in this organism have revealed a complex process that probably includes bidirectional replication from origins (reviewed in Lecrenier and Foury, 2000) and/or rolling-circle type replication (Maleszka *et al*., 1991), which may be involved in creating concatamers that are transmitted to developing buds during asexual reproduction (Ling and Shibata, 2002, 2004).

Mitochondrial DNA in yeast cells is found in nucleoids, membrane-associated DNA–protein complexes (Williamson and Fennell, 1979; Miyakawa *et al*., 1987) that are responsible for mitochondrial segregation (Azpiroz and Butow,

1993; Nunnari *et al*., 1997) and are the sites of mtDNA replication (Meeusen and Nunnari, 2003). At least 20 different proteins can be cross-linked to mtDNA (Kaufman *et al*., 2000), including the soluble DNA-binding proteins Rim1p (single-stranded DNA-binding protein), Abf2p, a high-mobility group protein involved in maintenance, segregation, recombination and copy number control of mtDNA (Diffley and Stillman, 1991; Zelenaya-Troitskaya *et al*., 1998; MacAlpine *et al*., 1998) and Mgm101p, which may be involved in repair of oxidative damage to DNA (Meeusen *et al*., 1999). An intriguing subset of mtDNA-associated proteins are bifunctional (Kaufman *et al*., 2000), including Ilv5p, an acetohydroxyacid reductoisomerase that links amino acid starvation to nucleoid number (Zelenaya-Troitskaya *et al*., 1995; MacAlpine *et al*., 1998), and mitochondrial aconitase, a protein that may be a key link between mitochondrial metabolism and mtDNA maintenance, in addition to its enzymatic role in the Kreb's cycle (Chen *et al*., 2005).

Nucleoids are physically associated with the mitochondrial inner membrane, but a nucleoid-specific, inner membrane component has yet to be identified. A subset of nucleoids are associated with the integral outer membrane protein Mmm1p (Hobbs *et al*., 2001), suggesting a 'two-membrane spanning complex' (TMS; Meeusen and Nunnari, 2003). A mtDNA binding protein, Mgm101p (Meeusen *et al*., 1999), and Mip1p, the mitochondrial DNA polymerase, are also associated with the TMS (Meeusen and Nunnari, 2003). Recently, a second outer membrane protein, Mmm2p, was identified that is also associated with nucleoids, but appears to be part of a complex distinct from that harbouring Mmm1p (Youngman *et al*., 2004).

Mip1p is a member of the subclass of gamma (γ) or mtDNA polymerases within the family A group of DNA polymerases (Ito and Braithwaite, 1990; Blanco *et al*., 1991). Within the polymerase domain of these enzymes exist three conserved sequence motifs: Pol A, Pol B and Pol C (Ito and Braithwaite, 1990; reviewed in Kaguni, 2004; Figure 1A) and a proofreading $3'-5'$ exonuclease domain characterized by three conserved sequence motifs, viz. Exo I, Exo II and Exo III (Bernad *et al*., 1989), all of which are present in the mitochondrial enzymes (reviewed in Kaguni, 2004; Figure 1A). MtDNA polymerases can be differentiated from other members of family A based on four conserved signature sequences ($\gamma 1-\gamma 4$) that are located within a 'spacer region' between the exonuclease and polymerase domains, and two regions ($\gamma 5$ and $\gamma 6$) that flank the carboxyl-terminal polymerase motif (Pol C, Figure 1A). Conserved sequence elements $\gamma 1$, $\gamma 3$ and $\gamma 4$ may function as part of the polymerase catalytic domain; the roles of $\gamma 5$ and $\gamma 6$ have not been investigated (Luo and Kaguni, 2005).

In comparison with the other γ polymerases, there are two remarkable features of the yeast enzyme: the apparent lack of an accessory subunit (e.g. Vanderstraeten *et al*., 1998) and the presence of a long extension to the C-terminal side of the $\gamma 6$ region (Foury, 1989; Figure 1). γ polymerases from *Drosophila* (Olson *et al*., 1995), *Xenopus* (Insdorf and Bogenhagen, 1989), mouse (Johnson *et al*., 2000) and humans (Gray and Wong, 1992) consist of a catalytic core and an accessory subunit, which stimulates catalysis and increases the processivity of the catalytic core (reviewed in Kaguni, 2004). The carboxyl-terminal regions of the accessory subunits resemble class IIa aminoacyl-tRNA synthetases, suggesting a role for RNA primer binding during initiation of mtDNA synthesis (Carrodeguas and Bogenhagen, 2000; Carrodeguas *et al*., 1999, 2001; Fan *et al*., 1999; Fan and Kaguni, 2001; Iyengar *et al*., 2002).

The C-terminal extension (CTE) on the fungal enzymes has remained enigmatic. The only clue to its function was the analysis of a yeast mtDNA polymerase harbouring a single amino acid substitution at residue 1001 of the preprotein (Hu *et al*., 1995). Cells harbouring this mutant form respiratory incompetent *petites* at increased levels and have a 50–60-fold increase in the frequency of erythromycin-resistant cells, indicative of mtDNA point mutations in the 21S rRNA gene (Hu *et al*., 1995).

Using the genome sequence data now available, we have carried out a more comprehensive search for CTEs in mtDNA polymerases, analysed the distribution of these sequences and examined them for conserved features. Based on the resulting information, C-terminal truncation variants of Mip1p were generated and the ability of cells harbouring these mutant polymerases to replicate and maintain mtDNA was analysed.

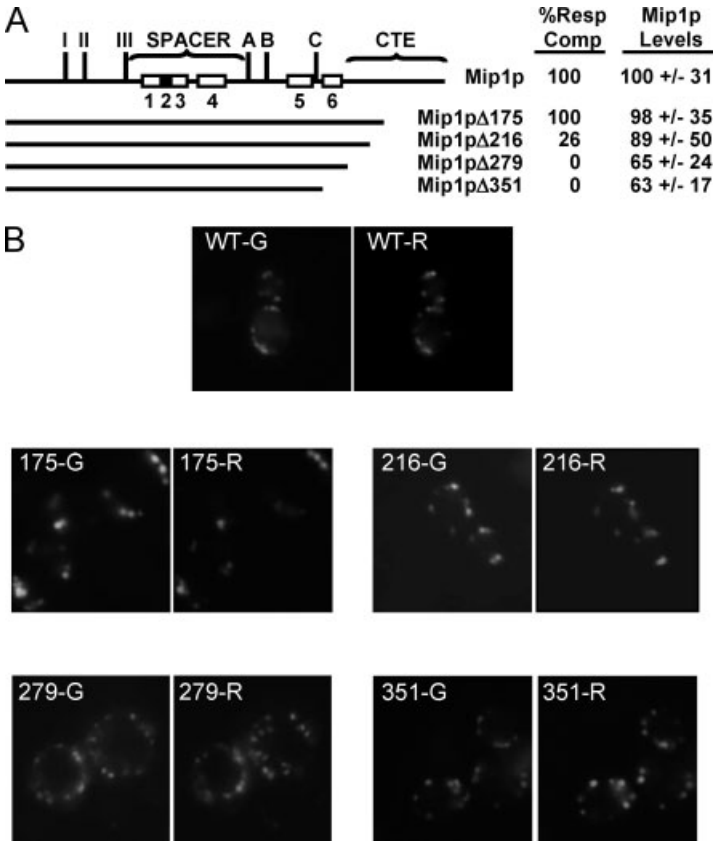

Figure 1. Schematic diagram of the wild-type Mip1p (top line) and four truncation variants. I, II, and III indicate the location of the three conserved exonuclease motifs that define the 3′–5′ exonuclease domain, while A, B and C indicate the location of the three conserved polymerase motifs that define the polymerase domain (Kaguni, 2004). Boxes numbered 1–6 in the wild-type Mip1p indicate the positions of the mtDNA polymerase γ-specific sequences. The locations of γ1–γ4 are taken from Luo *et al.* (2005); γ5 and γ6 comprise residues 805–876 and 905–959, respectively, of the Mip1p preprotein (Kaguni LS, personal communication). The γ2 sequence is shaded black to clearly delineate it from γ1 and γ3. 'CTE' indicates the location of the carboxyl-terminal extension unique to fungal polymerases. Variants with truncations in this region are indicated below. The % Resp Comp column indicates the percentage of between 36 and 67 independent transformants of each strain that were able to respire after transfer from the initial SC – HIS plate to YPG plates. The 'Mip1p level' column indicates the relative levels of the Mip1p variants, determined as described in Materials and methods. The value for wild-type Mip1p was arbitrarily set to 1. (B) Fluorescence of Mip1p–GFP variants. The left- and right-hand panels show Mip1p–GFP (G) and mitochondrial dsRED (R) fluorescence, respectively, from the same field of view. Truncation variants are indicated by the number of amino acid residues removed from the C-terminus; WT indicates wild-type cells. Images obtained from 0.2 μm slices are presented

Materials and methods

Strains and growth conditions

S150 (*leu2-3,112*, *his3-Δ1, trp1–289, ura3-52*; Steger *et al.*, 1990) was the wild-type strain used for expression of Mip1p truncation variants in this study. Yeast were grown on various media including: YPG (1% yeast extract, 2% peptone, 3% glycerol); YG-Er (2% yeast extract, 3% glycerol, 50 mM potassium phosphate, pH 6.5, 4 g/l erythromycin); YP2D (1% yeast extract, 2% peptone, 2% dextrose); YP10D (1% yeast extract, 2% peptone, 10% dextrose); YPL (1% yeast extract, 2% peptone, 2% lactic acid, pH 5.2); SC – HIS (0.67% Difco™ nitrogen base without amino acids, 4% dextrose, all amino acids except histidine, pH 5.6).

Strain construction

Mutant versions of the mtDNA polymerase gene were generated by site-directed mutagenesis

(Kunkel *et al*., 1987), using the Muta-Gene kit from Bio-Rad (Mississauga, Canada). Base pairs (bp) and amino acid residue numbers refer to the 1254-residue protein that would be encoded from the start codon downstream of the transcriptional start point identified by Foury (1989). The template DNA was obtained from plasmid pBluescript::*MIP1*-F3, which contains bp 2538–3762 of the coding sequence for the Mip1p preprotein and extends 31 bp past the stop codon. Primers were used to introduce a stop codon (shown in bold) followed by a *Bgl*II site (shown underlined) for insertion of the selectable marker *HIS3* into the *MIP1* gene. The stop codons were introduced at positions 3114, 2925 and 2709 of the *MIP1* coding sequence to create the genes *mip1*Δ216, *mip1*Δ279 and *mip1*Δ351, respectively. The primers used for the site-directed mutagenesis were synthesized by Canadian Life Technologies Inc. (Burlington, Canada) and are as follows: for *mip1*Δ351, 5′-GCGAAAAGGACAAA**TAG**ATCTCAGAGCTG-CTATGG; for *mip1*Δ279, 5′-ATCAATCAACTG-CTA**TAG**ATCTGACAAATCCAATAG; and for *mip1*Δ216, 5′-GGCTAGAAGATGAG**TAG**ATCT-GCGGGAGTGTAC.

The sequences of the regions to be expressed as part of the mutated polymerases were confirmed by DNA sequencing. After mutagenesis, the *Bgl*II site was used for the insertion of a *Bam*HI fragment containing the *HIS3* gene. The mutated sequences were released from pBluescript SK$^-$ by double digestion with *Xba*I and *Pvu*II, followed by gel purification using the QIAquick® Gel Extraction Kit (QIAGEN Inc., Mississauga, ON). Mutated fragments were then transformed into S150 yeast cells using the lithium acetate method (Gietz *et al*., 1997). Insertion of the truncation cassette at the correct position was first confirmed by colony PCR according to Sambrook and Russell (2001), except that the colony was first resuspended in water and then diluted into a standard PCR reaction mixture containing 3.1 mM $MgSO_4$. The primers used correspond to bp 2585–2605 of the *MIP1* open reading frame for the upstream primer and 11–31 bp downstream of the wild-type stop codon for the downstream primer. Southern blot analysis using a *MIP1*-specific probe was carried out to confirm correct isolates identified by colony PCR.

To create the coding sequence for *mip1*Δ175, a *HIS3* marker was ligated into the *Bam*HI site (position 3232 bp of the *MIP1* gene) in *MIP1*-F3 cloned in pAS1 (Gietz *et al*., 1997). The resulting disruption construct was transformed into S150 yeast and confirmed as described above. The *mip1*Δ175 construct encodes an additional 10 C-terminal amino acids (AARSCSLACT) due to the extension of the reading frame into the *HIS*3 cassette.

Green fluorescent protein (GFP)–Mip1p fusions were created as described by Sheff and Thorn (2004). The template for PCR was the pKT128 vector containing the yEGFP open reading frame and the *SpHIS5* marker, obtained from EUROSCARF. The following *MIP1*-specific sequences were included in the primers; [F5] and [R3] refer to the template-specific segments of the primers (Sheff and Thorn, 2004):

Mip1pΔ351, 5′-CCATGATGAGATTAGATTTTT-GGTGAGCGAAAAGGACAAA[F5]
Mip1pΔ279, 5′CATTCCTCATGGGGAGGCGCT-TGATATCAATCAACTGCTA[F5]
Mip1pΔ216, 5′-CCAGTCAGATAAGCGCGATG-TGAATCGGCTAGAAGATGAG[F5]
Mip1pΔ175, 5′-CGAGAAGGGCAAAAGGACT-AAAGTACGTATTATGGGATCC[F5]
Mip1p, 5′-GGTTGAGCTGGAAAGGGACATTA-CTATTTCTAGAGAGTAC[F5]
Mip1p Reverse (used for all constructions), 5′-TAATGTGCTGTATATATAAATACAAATGC-GAAAGCTAATG[R3]

The resulting PCR products were transformed into wild-type S150 cells according to Gietz *et al*. (1997). Colony PCR was used to confirm the upstream and downstream recombination junctions and the absence of the wild-type *MIP1* allele. Maintenance of respiratory function was indistinguishable in the wild-type cells and those expressing Mip1p–GFP, as observed by others (Meeusen and Nunnari, 2003). To visualize mitochondria, the resulting cells were transformed with pVT100U::dsRED, which encodes a mitochondrially targeted dsRED fluorescent protein (Meeusen and Nunnari, 2003).

Fluorescence microscopy of cells harbouring Mip1p–GFP fusions

A Zeiss Axio Imager Z1 was used for fluorescence microscopy and images were collected with

an AxioCam Mrm camera. For each field, *z*-stacks of four 0.2 μm slices were obtained. The fluorescence of the Mip1p–GFP variants was normalized to the emission from the mitochondrial dsRED, which is imported into mitochondria in the absence of mtDNA (Wong *et al*., 2000). To avoid bias toward mitochondria with GFP fluorescence, 15–20 mitochondrial puncta, in at least three different cells, were chosen based on dsRED fluorescence only. Fluorescence was then measured in the red and green channels separately, corrected for exposure time and summed for the entire stack. These values were used to calculate a ratio of Mip1p–GFP (green) to mitochondrial (dsRED) fluorescence. The ratio for the wild-type cells was set to 1.

Assessment of mtDNA maintenance and replication fidelity

Respiratory competence was monitored over 96 h. Yeast were first grown in YPL broth for 48 h to ensure a 100% respiring culture. Cultures were then diluted to 0.01 OD_{600nm}/ml YP10D broth for growth with shaking at 30 °C. Subsequently, cultures were diluted to 0.01 OD_{600nm}/ml every 24 h and glucose levels were continually monitored (Young and Court, 2004) to ensure sufficient (>1%) glucose to avoid selection of respiratory-competent cells.

Slides for fluorescence microscopy of 4′,6-diamidino-2-phenylindole (DAPI)-stained cultures were prepared to monitor the presence of mtDNA during growth. Cultures were diluted to 0.7 OD_{600nm}/ml in 5 ml YP10D broth and DAPI was added to a final concentration of 2.5 μg/ml. Cultures were incubated for 40 min with shaking at 30 °C, followed by washing with double-distilled water and resuspension in a 1/5 dilution of YP10D. The DAPI-stained culture was combined with an equal volume of 0.7% low gelling agarose (Mandel, Guelph, ON) made in double-distilled water, followed by visualization using Zeiss epifluorescent microscopy. At the indicated time points, cells were removed, diluted appropriately and spread onto YP2D plates to determine the number of viable cells. The resulting colonies were overlayed with 2,3,5-triphenyl tetrazolium chloride agar according to Ogur *et al*. (1957). Respiratory competence was calculated as the number of red, respiring colonies divided by the total number of colonies multiplied by 100.

Southern blot analysis was used to estimate relative content of intact mtDNA. Cells were harvested by centrifugation from the same cultures used for DAPI-staining and frozen at −60 °C until used for genomic DNA preparation (Philippsen *et al*., 1991). A 980 bp region of the mitochondrially-encoded *COX2* locus (bp 52 of the *COX2* ORF to 275 bp past the stop codon) was cloned into pBluescript SK^- and used as a template for generation of a digoxigenin-labelled DNA probe (Roche, Laval, PQ). A 1.5 kb *Hin*dIII genomic fragment harbouring the nuclear *RIM1* gene (a generous gift of F. Foury, Université Catholique de Louvain, Belgium), was gel-purified and used to generate a nuclear DNA probe. Hybridization was carried out as described by Roche.

Erythromycin-resistance was monitored according to Hu *et al*. (1995) with the following modifications. 3.3–13.3 OD_{600nm} units (ca. $1–4 \times 10^8$ cells) were spread onto YG-Er plates from an overnight culture grown in 20 ml of a 50 : 50 mixture of YPG : YP2D. Appropriate dilutions were also spread onto YPG plates to determine the actual number of respiratory-competent cells on the YG-Er plates. This step was necessary due to the generation of a high number of spontaneous *petites* by *mip1Δ216* strains.

Phylogenetic analyses

A total of 25 sequences (Table 1) were aligned with ClustalX (Thompson *et al*., 1997) and alignments were manually edited with GeneDoc v 2.5.010 (Nicholas and Nicholas, 1997). The amino-terminal sequences (*S. cerevisiae* residues 1–37), containing the putative mitochondrial targeting signals, and most of the CTEs (residues 1007–1254) aligned poorly and were removed. In addition, short gaps were introduced by ClustalX to several sequences to maintain the overall alignment; the resulting non-informative positions were also removed. These positions correspond to residues 61–67, 204, 388, 476, 531–537, 548, 551, 596–638 and 987–988 of the *S. cerevisiae* mtDNA polymerase. Parsimony, maximum likelihood (ML), and neighbour-joining (NJ) phylogenetic analyses of the mtDNA polymerase sequences were carried out using the appropriate programs contained within PHYLIP (Felsenstein, 2002). PROTDIST was used in combination with NEIGHBOUR to generate the tree presented in Figure 2. The data

Table 1. Sources of mitochondrial DNA polymerase primary sequences used for phylogenetic analyses

Organism	Accession No.[a]
Metazoans	
Drosophila melanogaster	AAF53338
Homo sapiens	AAH50559
Ascomycetes	
Aspergillus fumigatus	Contig 41 at: **http://www.genedb.org/genedb/asp/** 665938–662894
Aspergillus nidulans	EAA65359
Candida albicans	AACQ01000065 Translation of nucleotides 77331–81017
Candida glabrata	CAG58839
Cryptococcus neoformans var. *grubii*	AACO01000141 Translation of nucleotides 185165–183051, 183048–182818 and 182815–181124[b]
Debaryomyces hansenii	CAG89264
Eremothecium gossypi	AAS52277
Gibberella zeae	EAA74646
Histoplasma capsulatum	HISTO_LF.Contig359 at: **www.genome.wustl.edu/blast/histo_client.cgi** Translation of nucleotides 555043–558543
Kluyveromyces lactis	CAG97904
Kluyveromyces waltii	AADM01000080 Translation of nucleotides 54465–58145
Magnaporthe grisea	EAA46570
Neurospora crassa	AAD21034.1
Phanerochaete chrysosporium	Protein Id 23153 *Phanerochaete chrysosporium*: gw.121.2.1
Pichia pastoris	AAB17118.1
Podospora anserina	Contig_824 at: **http://podospora.igmors.u-psud.fr** Translation of nucleotides 3994–7461
Saccharomyces bayanus	AACA01000477 (Partial[c]) Translation of nucleotides 3–3749
Saccharomyces castellii	AACF01000124 (Partial) Translation of nucleotides 2–3316
Saccharomyces cerevisiae	CAA99652.1
Saccharomyces kluyveri	AACE01000598 (Partial) Translation of nucleotides 1380–2267
Saccharomyces kudriavzevii	AACI01000043 (Partial[d]) Translation of nucleotides 2811–34
Saccharomyces paradoxus	AABY01000003 Translation of nucleotides 136136–132363
Schizosaccharomyces pombe	CAA88012
Yarrowia lipolytica	CAG78428

[a] Accession numbers refer to predicted amino acid sequences, with the exception of those that were generated by conceptual translation of the indicated nucleic acid sequence and are therefore indicated as 'translation of nucleotides'. The positions given include the putative stop codon.

[b] The indicated contig, when translated, contained three segments detected by TBLASTN as being similar to known mitochondrial DNA polymerases. Each of the three segments was in a different reading frame; hence a putative mtDNA polymerase reading frame was estimated by introducing two 2 bp deletions, as indicated.

[c] Partial indicates that a reading frame encoding only part of the expected sequence of a mtDNA polymerase was identified. Partial sequences were only used in the analysis in Figure 2A if the entire putative 3′–5′ exonuclease and polymerase domains could be identified.

[d] The *S. kudriavzevii* sequence data was used only for the alignment in Figure 2B, as only the 3′ sequence, including the polymerase domain and the CTE, were available.

were then processed through the bootstrap procedure (Felenstein, 1985; SEQBOOT, 1000 replicates). The resulting bootstrapped replicate-based phylogenetic estimates were evaluated using PROTDIST, NEIGHBOUR and finally CONSENSE to obtain the level of support for the nodes

in the NJ tree. Likewise, the bootstrapped dataset was analysed with PROTPARS and PROML to obtain support for parsimony and ML phylogenetic trees.

The PRALINE online server (**http://ibivu.cs.vu.nl/programs/pralinewww/**; Simossis and Heringa, 2003) was employed for the multiple sequence alignment and secondary structural predictions outlined in Figure 2.

Results and discussion

Phylogenetic analysis of fungal mitochondrial DNA polymerases

Carboxyl-terminal extensions were first noted on the mtDNA polymerases of *Saccharomyces* (Hu *et al*., 1995) and *Neurospora* (Ko T, Bertrand H, personal communication; see Table 1). With the wealth of new genome sequence data, it was possible to both investigate the phylogenetic relationships among mtDNA polymerases and determine the presence of CTEs among the taxonomic groups. The focus of this study was the Ascomycota, including members of the Pyrenomycetes, the Plectomycetes and yeast-like representatives. Mitochondrial DNA polymerase sequences from the club fungi, the Basidiomycota, and the metazoans, *Drosophila melanogaster* and *Homo sapiens*, were used as outgroups. The latter two enzymes do not possess C-terminal extensions (Figure 2A); therefore, the core regions of the polymerase sequence, encompassing the 3′–5′ exonuclease and polymerase domains were used for phylogenetic analyses (see Materials and methods).

ClustalX alignment of unambiguous positions, followed by parsimony, neighbour-joining and most-likelihood analyses, revealed evolutionary relationships among the mtDNA polymerases (Figure 2A) that mirrored those shown by similar analyses of both large (Dujon *et al*., 2004) and small (Cavalier-Smith, 2001) rDNA sequences. Notably, the metazoan enzymes are most distant from those of the fungi and those of the Basidiomycetes group separately from the Ascomycetes.

The CTEs of the various polymerases were defined as all residues to the C-terminal side of the core enzyme (residues 975–1254 of the *S. cerevisiae* Mip1p preprotein). The N-terminus of CTE therefore is 26 amino acids from the end of the predicted polymerase domain (Blanco *et al*., 1991) that terminates at residue 949 and includes the pol C motif (Figure 1). The CTE also extends 16 residues past the $\gamma 6$ region described by Kaguni (2004). The lengths of resulting CTEs are plotted alongside the phylogenetic tree (Figure 2A). Remarkably, the lengths of the CTEs do not correlate strictly with the phylogenetic positions of the organisms. For example, the CTE on the mtDNA polymerase of *Neurospora* is almost twice as long as that of the other pyrenomycete fungi. Similarly, within the tight grouping of *Pichia, Debaromyces* and *Candida*, the lengths of the CTEs vary (68–328 residues). Overall, several size classes are apparent: 'long' CTEs of about 280 residues found in *Neurospora* and some yeast-like fungi; 'medium length' CTEs of about 150 residues in filamentous fungi, *C. albicans*, and *Eremothecium*; and 'short' CTEs of less than 93 residues in the ascomycetes *Yarrowia, Schizosaccharomyces* and *Pichia*, as well as the basidiomycete *Cryptococcus*. CTEs in the polymerases from human, *Drosophila* and the white-rot fungus *Phanerochaete* are less than 22 residues in length.

BLAST searches of fungal CTEs do not reveal significant similarities with any known proteins (data not shown). Therefore, in an attempt to identify important features of CTEs, a multiple alignment of all CTEs was performed. No obvious conservation was observed across all polymerases. However, when CTEs from 10 representatives of the Saccharomycetales were aligned with PRALINE (Simossis and Heringa, 2003), a gradient of sequence relatedness was observed, with most similarity near the polymerase domain (residues 10–69 of the alignment in Figure 2B). Some conservation is observed between residues 70 and 100, and the remaining sequences are unrelated (residues 101–150 in Figure 2B and data not shown). Only three residues are absolutely conserved, viz. arginine at position 29 of the alignment (R1001 of the Mip1p preprotein), glutamine at position 52 (Q1024) and lysine at position 99 (K1070). Once the function of the CTE is known in more detail, the precise role(s) of these residues can be addressed through the analysis of single-residue variants.

Truncation variants of *Saccharomyces* mtDNA polymerase

As an initial approach to determine the importance of the CTE of *S. cerevisiae* Mip1p, a series of

truncation variants was generated (Figure 1). The largest deletion, in Mip1pΔ351, leaves only five amino acids to the C-terminal side of the conserved HDEIRFLV motif in the Pol C domain (Kaguni, 2004). The segment removed includes 71 well-conserved positions, including the mtDNA polymerase-specific region, γ6, and therefore is likely to disrupt part of the polymerase domain. The truncation removes all of the CTE in Mip1pΔ279, and its terminus corresponds to the last residues shared between the fungal and metazoan mtDNA polymerases. Mip1pΔ216 retains most of the highly conserved region in fungal CTEs, while Mip1pΔ175 lacks only the highly variable C-terminal 63% of the CTE (see Figure 2B). The genes encoding the truncation variants were transformed into haploid S150 yeast to replace the wild-type *MIP1*.

Respiratory competence of *Mip1p* variants

Following selection for insertion of the *mip1* truncation mutations on SC − HIS plates, single colonies were tested for respiration. *mip1Δ351* cells rapidly lost respiratory competence; none of the 14 colonies taken directly from the transformation plates from two separate experiments grew on glycerol-containing medium (Figure 1). Furthermore, mtDNA was not detected in these cells by DAPI staining (data not shown). These results confirm that the entire polymerase domain, including γ6, is required for mtDNA polymerase function. The initial cells used for the transformation could respire, as indicated by the respiratory ability of transformants in which the *HIS3* marker in the *mip1* truncation plasmids had successfully recombined into the *his3Δ1* locus (data not shown). In general, these *HIS*$^+$ cells produced large colonies on the transformation plates, while recombination into the *MIP1* locus gave rise to small colonies. Similarly, 14/14 *mip1Δ279* colonies obtained from two independent transformations were respiratory-incompetent (Figure 1) and mtDNA staining was not detected (data not shown). This variant retains all of the residues conserved between fungal and metazoan polymerases, indicating that all or part of the CTE is required for mtDNA maintenance in yeast.

To confirm that these two variant polymerases were imported into and maintained in mitochondria, fluorescence microscopy of cells harbouring fusions of GFP to the truncated C-terminal end of Mip1p was performed. These transformants lacked the ability to respire, as did their *mip1Δ279* and *mip1Δ351* counterparts. In both Mip1pΔ279–GFP and Mip1pΔ351–GFP strains, green fluorescence co-localized with red fluorescence from mitochondrially targeted dsRED (Figure 1B). Assuming that any reduction in mitochondrial import in *petite* cells would affect the import of both proteins equally, the ratios of GFP and dsRED fluorescence were used to estimate the mitochondrial levels of the Mip1p variants relative to that of the wild-type protein (Figure 1A). The average levels of both truncation variants were lower than that of wild-type protein but, given the standard deviations in

Figure 2. Phylogenetic analysis of mtDNA polymerases. (A) Phylogenetic analysis of the 'core' polymerase region, including the exonuclease and polymerase domains. Analysis was carried out as described in Materials and methods. Taxa are colour-coded: metazoans (mz, red), *Schizosaccharomyces pombe* (green), *Saccharomycetales* (*Sa*, grey), plectomycete fungi (pl, blue), pyrenomycete fungi (py, purple) and basidomycetes (ba, brown). Nodes that received support from bootstrap analysis, when combined with NJ, ML and parsimony analyses above 95%, are indicated by an asterisk, above 85% by # and above 75% by +. For lower levels of support, NJ values are indicated; ML and parsimony values are presented in square brackets and parentheses, respectively. A schematic map to the right of the phylogenetic tree shows the lengths of the CTEs for the various polymerases. The CTE has been designated as the sequence 26 residues past the end of the predicted polymerase domain (Blanco *et al.*, 1991); this encompasses residues 975–1254 of the *S. cerevisiae* preprotein. The contig containing the *S. kudriavzevii MIP1* gene contains the entire sequence used for the alignment but ends before the coding sequence for the CTE; hence, the length of the CTE is listed as unknown. (B) Comparative analysis of predicted CTE sequences. An alignment of the CTEs was generated using PRALINE (Simossis and Heringa, 2003), and conservation scores and predicted secondary structures for various yeast CTEs are presented. 'Consistency' refers to how consistently an amino acid is found at a given position in the final multiple alignment and in pre-processed alignment blocks (Heringa, 1999). In the 10-point consistency scale, zero (purple) indicates the least conserved alignment position, while * (red) indicates the most conserved positions. Only the first 150 positions of the 328-residue alignment are shown, because the overall similarity among the C-terminal segments is very low. The solid and dashed lines indicate long and short structural features that are predicted in at least 8 of 10 sequences. The positions of the various truncations are indicated at the top of the alignment

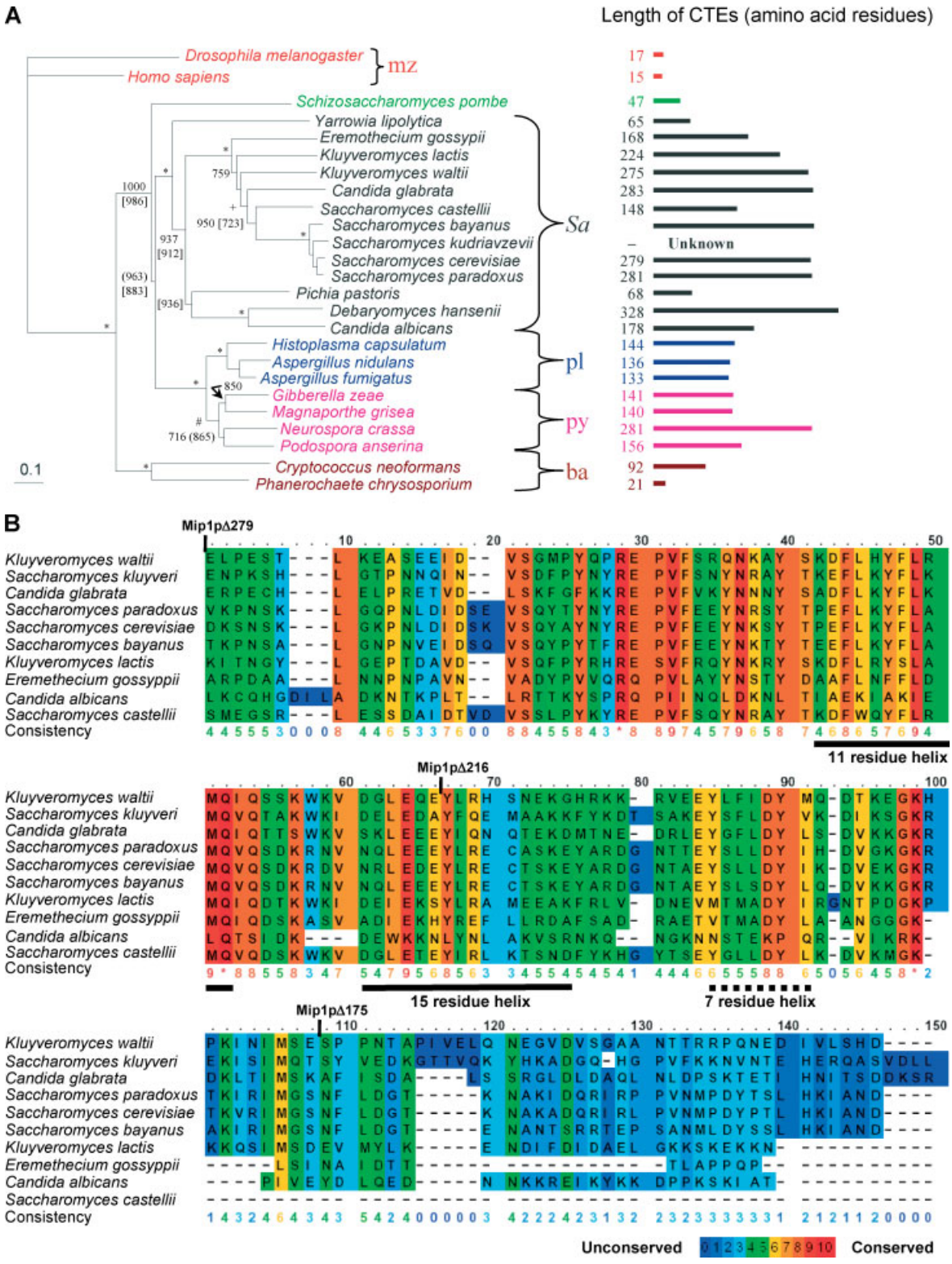

each dataset, these differences are not statistically significant. Thus, the defects in *mip1Δ279* and *mip1Δ351* cells are not likely the result of severely reduced levels of mtDNA polymerase; a stabilizing effect of the GFP moiety cannot be ruled out.

mip1Δ216 transformants were of two types: those unable to respire and those that showed weak growth on glycerol-containing plates; the polymerase levels were again similar to those in wild-type cells (Figure 1A). Therefore, the inclusion of residues 975–1038 only partially compensates for the lack of function in Mip1pΔ279, and the C-terminal GFP fusion does not affect the phenotype. To further analyse the poorly respiring *mip1Δ216* cultures, respiratory competence was assessed after growth in glucose, which is non-selective for mtDNA function. Under these conditions, *mip1Δ216* cells rapidly lost respiratory competence; after 24 h growth, approximately 2% of the colonies could respire. In contrast, about 99% of the wild-type cells were respiratory-competent (data not shown).

mip1Δ175 transformants produced large, respiratory-competent colonies. After 4 days growth in glucose, almost all cells retained respiratory competence (98.2%) and mtDNA staining (100% of 77 cells), and levels of Mip1pΔ175–GFP were similar to those of Mip1p–GFP in wild-type cells (Figure 1A). Therefore, replacement of the terminal part of the CTE with another protein does not alter the wild-type phenotype. As *mip1Δ175* cells were indistinguishable from wild-type, the entire CTE is not required for mtDNA maintenance, and further truncations in the C-terminal region of the CTE were not made.

Mutator phenotype of *mip1Δ216* cells

The *mip1Δ216* mutant was ideal for further analysis because it was capable of long-term respiratory growth on media containing non-fermentable carbon sources, indicating that it maintained functional mitochondrial genomes. Therefore, it was possible to assess the defects associated with this truncated polymerase. There are several possible reasons for the loss of respiratory competence in *mip1Δ216* cells: complete loss of mtDNA, major deletions and rearrangements of the mitochondrial genome, or multiple point mutations.

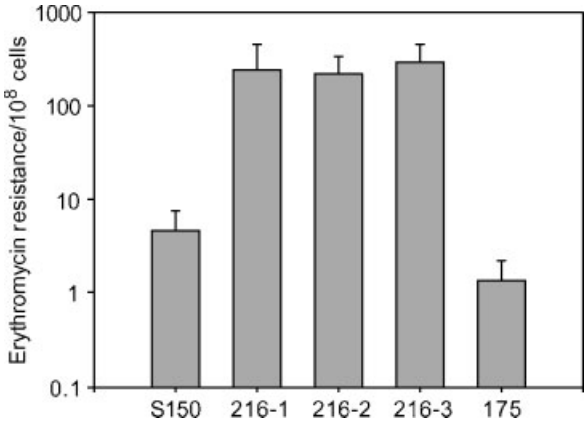

Figure 3. Point mutations in mtDNA. The relative fidelity of mtDNA replication in wild-type (S150) and *mip1Δ175* (175) cells was assessed as the frequency of erythromycin-resistant colony formation per 10^8 cells, as described by Hu *et al.* (1995). Each strain was analysed in triplicate and averages and standard deviations are presented. Data obtained for three independent isolates of *mipΔ216* (216-1, 216-2, 216-3) are presented

Because *mip1Δ216* cells can maintain mtDNA under selective pressure, fidelity of mtDNA replication can be investigated using the erythromycin-resistance assay (Hu *et al.*, 1995). Cultures of wild-type S150 cells produced 2–8 erythromycin-resistant colonies/10^8 cells (Figure 3), in the same order of magnitude as observed by Hu *et al.* (1995) for W303-1B. Resistant *mip1Δ175* cells appeared at the same frequency, indicating that the 175 C-terminal residues are not involved in replication fidelity. However, each of three independent *mip1Δ216* transformants produced highly variable levels of resistant cells in replicate experiments; overall there were 10–100 times more resistant cells than seen for the wild-type control (Figure 3). These observations suggest that the Mip1pΔ216 polymerase is more error-prone than the wild-type enzyme. The level of erythromycin-resistance acquired by *mip1Δ216* cells was similar to that observed for mtDNA polymerases, with point mutations in the proofreading $3' \rightarrow 5'$ exonuclease domain (Hu *et al.*, 1995). For the latter mutants high variation between experiments was also observed. In the case of *mip1Δ216* cells, this variation likely reflects the reduced mtDNA copy number (see below). Assuming most mutations occur in the YPD culture of each isolate prior to plating on erythromycin, cells with a low number of mtDNA molecules would

have an increased probability of transmitting an erythromycin-resistant genome to their progeny cells. Therefore, the number of resistant cells in the culture would be greatly influenced by when the mutation occurred — early or late. The variation in total mtDNA levels among the isolates (see below) would compound this effect.

Loss of mitochondrial DNA in *mip1*Δ*216* cells

Mitochondrial DNA maintenance by *mip1*Δ*216* cells was investigated during non-selective growth on glucose, using both DAPI staining of whole cells and Southern blot analysis (Figure 4). Cultures were first grown in lactate to ensure respiratory activity at the start of the experiment. DAPI staining is most effective in glucose-grown cells (data not shown); therefore all cells were exposed to glucose for 40 min during staining. After staining, almost all wild-type and *mip1*Δ*216* cells taken directly from the YPL culture showed strong, punctate mtDNA staining in the periphery of the cell (Figure 4A). However, the *mip1*Δ*216* cells usually contained fewer nucleoids (one to three per focal plane) than did the wild-type (at least five). For the wild-type cells, the staining pattern remained virtually unchanged through almost 22 h of growth in glucose (Figure 4A). However, the number of *mip1*Δ*216* cells with DAPI mtDNA staining was drastically reduced (to 29.3%) after only 5.4 h of growth and none of the cells showed staining after 22 h (Figures 4A, 5A). This trend was observed in the three strains, each derived from an independent *mip1*Δ*216* transformant. In similar experiments, wild-type and *mip1*Δ*175* cells maintained high levels of mtDNA staining during 96 h of growth in glucose (data not shown).

The loss of intact mtDNA was confirmed by Southern blot analysis (Figure 4B) of wild-type and *mip1*Δ*216* cells. Following initial growth in YPL, whole cell DNA from both strains contained a single *Sac*II fragment detected by a probe for the mitochondrial gene *COX2*. However, compared to the signal for the nuclear gene *RIM1*, the relative amount of intact mtDNA in the *mip1*Δ*216* cells was about one-third that of the wild-type (Figures 4B, 5A), in agreement with the DAPI staining. During non-selective growth on glucose, the three independent *mip1*Δ*216* strains rapidly lost *COX2* hybridization (Figure 4B shows a representative). These results also indicate that the

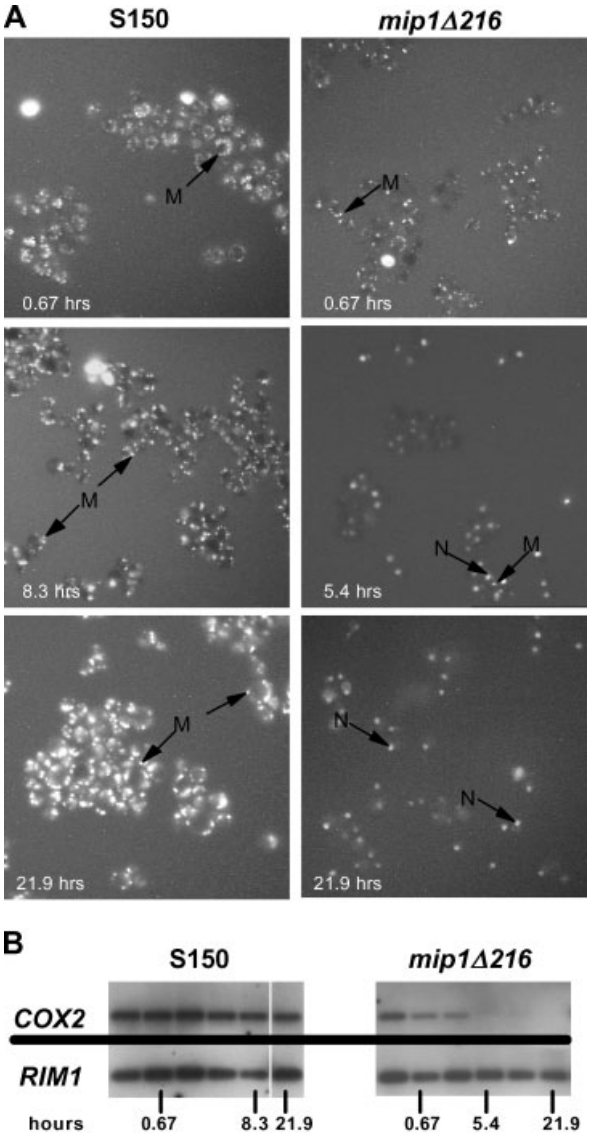

Figure 4. Time-course analysis of mtDNA maintenance. Each experiment was performed with three independent *mip1*Δ*216* or S150 isolates and a representative experiment is shown. (A) DAPI staining. S150 and *mip1*Δ*216* cells were grown under non-selective conditions (YP10D). The presence of mtDNA was assessed by DAPI staining of cultures at the indicated time points, which include the 40 min of the staining procedure. M, punctate mitochondrial staining; N, nuclear staining. Nuclear staining is relatively weak in cells with strong mitochondrial signals. (B) Southern blot analysis. Whole-cell DNA was isolated from S150 (left) and *mip1*Δ*216* cells (right) immediately after transfer to YP10D (0 h) and following 0.67, 2.7, 5.4, 8.3 and 21.9 h growth in YP10D. DNA was then digested with *Hin*dIII and *Sac*II and analysed by Southern blot, using probes for mtDNA (*COX2*) and nuclear DNA (*RIM1*)

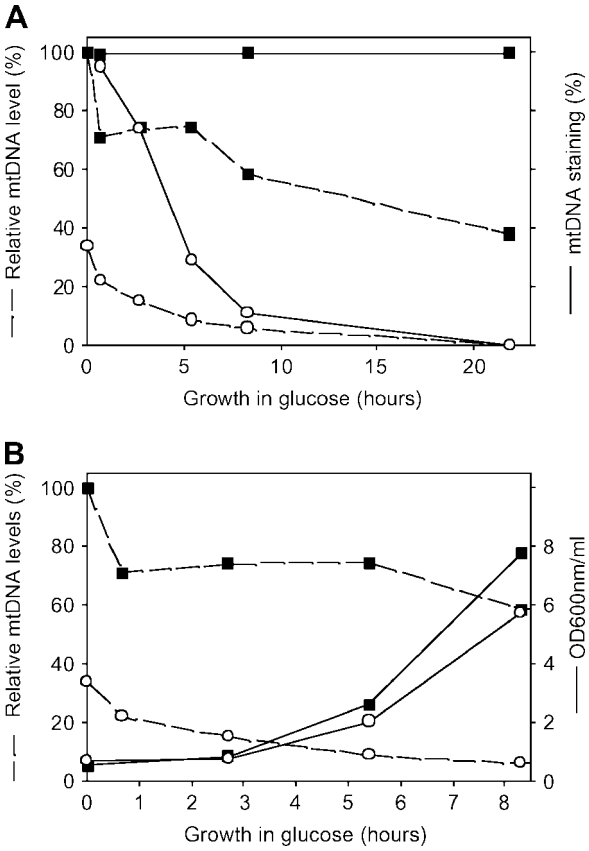

Figure 5. Quantitative analysis of mtDNA loss and growth rate. (A) The percentage of cells with mtDNA DAPI staining (solid line) and the relative levels of mtDNA (dashed lines) are presented for the S150 and *mip1*Δ*216* isolates shown in Figure 4. Comparative mtDNA levels were estimated from the ratio of the *COX2* to the *RIM1* signals (see Figure 4B). The ratio for the S150 cells grown overnight in YPL was set to 1 and used to standardize relative mtDNA levels for both S150 (filled squares) and *mip1*Δ*216* (open circles) cells during the time course. (B) mtDNA loss during cell division. The solid lines indicate the growth of the cultures used for Figure 4, and dashed lines the relative mtDNA levels. Growth was assessed spectrophotometrically at 600 nm

*mip1*Δ*216* cells had not acquired suppressor mutations during their initial growth in YPL.

Together, the DAPI-staining and Southern blot data revealed mtDNA loss that paralleled the growth of the *mip1*Δ*216* culture (Figure 5B). After 0.67 h growth in glucose, the cells were in early lag phase. At this point, mitochondrial staining was observed in about 95% of the *mip1*Δ*216* cells, but the *COX2* hybridization signal was reduced from 34% of wild-type levels to only 22% (Figures 4B, 5B). Similarly, wild-type cells maintained 100% DAPI staining, and a similar reduction of about 30% in the relative level of mtDNA was observed. Thus, both cell types appear to undergo a reduction in relative mtDNA levels upon transfer to a fermentable carbon source. The cells were in stationary phase following growth in YPL and, upon transfer to fresh media, nuclear DNA replication during lag phase would result in a reduction in the ratio of mtDNA to nuclear DNA, if the rate of nuclear DNA replication exceeds that of mtDNA.

After 2.7 h growth in glucose, the cells were just beginning to emerge from lag phase; mtDNA staining was observed in only 74% of the *mip1*Δ*216* cells, in contrast to its presence in virtually all wild-type cells (Figure 5A). In comparison to the 0.67 h timepoint, the relative *COX2* hybridization signal was reduced from 22% to 15% of wild-type levels in the mutant cells, and remained unchanged at about 70% of the initial level in the S150 cells (Figures 4B, 5B). Smearing of the *COX2* hybridization band was not observed (Figure 4B, and data not shown), suggesting that large-scale DNA rearrangements do not accompany mtDNA loss, but the *COX2* signal is weak in the *mip1*Δ*216* DNA and minor alternative forms may not have been detectable.

In the exponential growth phase, the loss of mtDNA continued in parallel to the loss of DAPI staining in *mip1*Δ*216* cells (Figure 5B), suggesting a defect in replication rather than in mtDNA distribution. In the latter case, one would expect the maintenance of a few cells with multiple nucleoids resembling those observed at the 0.67 h timepoint. However, a reduction in the number of nucleoids per cell is obvious by 5.4 h (Figure 4A). Throughout the remainder of the experiment, cells were maintained in log phase (see Materials and methods) and a dilution effect was observed, in that the mtDNA levels in *mip1*Δ*216* cells decreased by about half with each cell division (Figure 5B). For example, in the representative experiment shown in Figure 4A, after 5.4 h the *mip1*Δ*216* cells had doubled, and the levels of mtDNA dropped from 15% (2.7 h) of wild-type levels to 8.7% (Figure 5B). Likewise, the fraction of cells with DAPI-stained mitochondria fell from 74% (2.7 h) to 29% (Figure 5A). These results suggest an almost complete failure of mtDNA replication in *mip1*Δ*216* cells. In contrast, throughout the experiment (21.9 h), multiple nucleoids were visible in all

of the wild-type cells, and mtDNA was maintained, albeit at reduced levels (70–40%; Figures 4B, 5A). Similarly reduced levels of mtDNA in glucose-grown *S. cerevisiae* cells has been described previously (Dujon, 1981).

mtDNA maintenance by *mip1Δ216* cells in non-fermentable carbon sources

The *mip1Δ216* cells have very different mtDNA maintenance profiles when grown in fermentable vs. non-fermentable carbon sources: rapid mtDNA loss vs. maintenance of low levels of mtDNA in all cells. This effect is not related to glucose repression, as similar rates of mtDNA loss are observed upon growth in the non-repressing, fermentable carbon source raffinose (data not shown). One explanation for this observation is derived from the growth rates of the wild-type and *mip1Δ216* mutant cells. In liquid culture, *mip1Δ216* cells grow more slowly when respiring (doubling time of 5.3 ± 0.6 h in YPG) than do the wild-type cells (3.6 ± 0.1 h). In glucose, both cell types grow rapidly, with doubling times of 2.2 ± 0.3 and 2.4 ± 0.3 h, respectively. The reduced respiratory growth rate of *mip1Δ216* cells reflects lower respiration and energy production due to the intrinsically lower levels of mtDNA. Interestingly, most *mip1Δ216* cells are *rho*$^+$ during growth on glycerol (Figure 4A, 0.67 h timepoint), suggesting efficient transmission of mtDNA to daughter cells. Perhaps the slower growth rate during respiration allows for sufficient replication by the compromised polymerase to ensure high enough mtDNA levels for transmission to daughter cells. In contrast, the rapid growth rate in glucose may be insufficient for replication and partitioning of limited amounts of mtDNA. Investigation of this question using *in organello* measurements of mtDNA replication rates is not practical for two reasons. First, the mutant cells appear to harbour near-wild-type levels of Mip1pΔ216 (Figure 1B), but have lower levels of mtDNA (Figures 4, 5); thus, the ratios of mtDNA to polymerase are different than in wild-type cells. Second, the relative levels of mtDNA are variable in different YPL cultures derived from a single isolate. For example, three cultures derived from a single *mip1Δ216* isolate contained 34–75% of wild-type levels of mtDNA, as determined by Southern blotting (data not shown). As a result, the polymerase : template ratio is not constant in the mutant cells and valid comparisons with the wild-type can not be made. Therefore, future approaches to this question will involve biochemical characterization of over-expressed, purified Mip1p variants on standardized templates.

Possible functions of the CTE

The data presented herein demonstrate that only the γ6-proximal 104 residues of the CTE (residues 975–1079) are sufficient for wild-type polymerase function. This region, maintained in Mip1pΔ175 but not in Mip1pΔ279, is the most highly conserved CTE segment among mtDNA polymerases of Saccharomycetales (Figure 2B), but it is not well-conserved among more distantly-related organisms. The sequence of this region does not contain any known motif or predicted secondary structure that reveals its potential function. Given the lack of predicted sequence similarity between the CTE and the accessory subunits of metazoan mtDNA polymerases, it is unlikely that the CTE likely functions in polymerase loading at primer–template junctions in the same manner as the metazoan proteins.

Examination of the fungal CTE sequences did reveal several salient features. All CTEs are very polar (47–71%) and their isoelectric points are 9 or higher, with exception of the CTEs from *Schizosaccharomyces* (4.4), *S. castellii* (5.0) and *Eremothecium* (4.5), suggesting that these extensions could be involved in non-specific mtDNA binding. An arginine residue equivalent to R1001 is also present in all ascomycete CTEs examined. Hu *et al*. (1995) determined that cells harbouring a point mutation converting this arginine to isoleucine produced *rho*$^-$ cells at increased frequency (20% at 28 °C). This polymerase also displayed a moderate mutator phenotype (50 erythromycin-resistant colonies/10^8 cells). Mip1pΔ216 includes this arginine but produces a more severe phenotype, indicating that residues C-terminal to 1038 also contribute to mtDNA maintenance and fidelity of replication.

Secondary structure predictions for the conserved segments of the ascomycete CTEs (Figure 2B) reveal three potential α-helical regions, one of which contains the conserved glutamine residue, Q1024. This putative helix is very hydrophobic, while the 15-residue helix (Figure 2B) contains 13 polar residues and the seven-residue helix is amphipathic. In Mip1pΔ216 the putative 15-residue helix is interrupted and the smaller C-terminal one is completely removed.

In addition to DNA binding, there are several other possible functions of the CTE. First, it may be required for folding or stability of the mtDNA polymerase. It was difficult to use temperature sensitivity of the Mip1pΔ216 polymerase to assess stability because mtDNA loss occurred so rapidly at 30 °C and was complete after 24 h at either 30 °C (Figure 4A) or 37 °C (data not shown). In contrast, *mip1Δ175* cells grew and maintained respiratory competence indistinguishably from the wild-type at 37 °C, indicating that the C-terminal segment of the CTE is not required for stability of the polymerase at 37 °C. An argument against a possible role in folding or stability is that the all of the Mip1p–GFP fusion variants co-localized with mitochondrial dsRED (Figure 1B), indicating that these proteins are stably maintained in mitochondria. However, stabilizing effects of the GFP moiety cannot be ruled out.

The CTE may be involved in protein–protein interactions with the mtDNA replication machinery, the nucleoid structure or the two-membrane spanning complex. Several yeast two-hybrid screens using Mip1p as bait (Uetz *et al*., 2000; Ito *et al*., 2000; Li and Court, unpublished results), have not revealed any putative mitochondrial interaction partners. An interaction with Bur2p was detected, but it is a cytosolic RNA polymerase II-binding protein, so the nature of the interaction is not clear (Hazbun *et al*., 2003). A bacterial two-hybrid screen revealed a more relevant interaction with Sed1p, which was subsequently shown to be required for maintenance of normal levels of Mip1p and mitochondrial genome integrity (Phadnis and Ayres Sia, 2004). Mip1p has been shown to co-localize with the TMS protein Mmm1p by fluorescence microscopy (Meeusen and Nunnari, 2003), but a direct interaction between the two proteins was not demonstrated. Future studies in our laboratory will include suppressor screens to identify putative interactions between the CTE of Mip1p and other components of the mitochondrial DNA replication machinery.

Acknowledgements

This work was supported by a Discovery Grant from the Natural Sciences and Engineering Research Council (NSERC 184227) to D.A.C., a University of Manitoba Graduate Fellowship to M.J.Y. and a Manitoba Health Research Graduate Fellowship to M.L. We gratefully acknowledge Dr E. Huebner and Mr A. Dufresne, University of Manitoba, for their enthusiastic assistance with the fluorescence microscopy, and Dr G. Hausner, University of Manitoba, for sharing his expertise in phylogenetic analysis and for a critical reading of the manuscript. The excellent technical assistance of Enisa Zildzic, Kristen Creek and Allison Land is also acknowledged. We also thank Dr J. Nunnari, University of California at Davis, for generously providing the pVT100U::dsRED plasmid, and Dr L. Kaguni, Michigan State University, for providing us with the positions of the γ-polymerase-specific motifs.

References

Azpiroz R, Butow RA. 1993. Patterns of mitochondrial sorting in yeast zygotes. *Mol Biol Cell* **4**: 21–36.

Bernad A, Blanco L, Lazaro JM, *et al*. 1989. A conserved 3′–5′ exonuclease active site in prokaryotic and eukaryotic DNA polymerases. *Cell* **59**: 219–228.

Blanco L, Bernad A, Salas M. 1991. MIP1 DNA polymerase of *S. cerevisiae*: structural similarity with the *E. coli* DNA polymerase I-type enzymes. *Nucleic Acids Res* **19**: 955.

Carrodeguas JA, Bogenhagen DF. 2000. Protein sequences conserved in prokaryotic aminoacyl-tRNA synthetases are important for the activity of the processivity factor of human mitochondrial DNA polymerase. *Nucleic Acids Res* **28**: 1237–1244.

Carrodeguas JA, Kobayashi R, Lim SE, *et al*. 1999. The accessory subunit of *Xenopus laevis* mitochondrial DNA polymerase gamma increases processivity of the catalytic subunit of human DNA polymerase gamma and is related to class II aminoacyl-tRNA synthetases. *Mol Cell Biol* **19**: 4039–4046.

Carrodeguas JA, Theis K, Bogenhagen DF, Kisker C. 2001. Crystal structure and deletion analysis show that the accessory subunit of mammalian DNA polymerase gamma, Pol gamma B, functions as a homodimer. *Mol Cell* **7**: 43–54.

Cavalier-Smith T. 2001. What are fungi? In *The Mycota VII Part A: Systematics and Evolution*, McLaughlin DJ, McLaughlin EG, Lemke PA (eds). SpringerVerlag: Berlin; 3–37.

Chen XJ, Wang X, Kaufman BA, Butow RA. 2005. Aconitase couples metabolic regulation to mitochondrial DNA maintenance. *Science* **307**: 714–717.

Diffley JF, Stillman B. 1991. A close relative of the nuclear, chromosomal high-mobility group protein HMG1 in yeast mitochondria. *Proc Natl Acad Sci USA* **88**: 7864–7868.

Dujon B. 1981. Mitochondrial genetics and functions. In *The Molecular Biology of the Yeast Saccharomyces. Life Cycle and Inheritance*, Strathern JN, Jones EW, Broach JR (eds). Cold Spring Harbor Laboratory Press: Cold Spring Harbor, NY; 505–635.

Dujon B, Sherman D, Fischer G, *et al*. 2004. Genome evolution in yeasts. *Nature* **430**: 35–44.

Fan L, Kaguni LS. 2001. Multiple regions of subunit interaction in *Drosophila* mitochondrial DNA polymerase: three functional domains in the accessory subunit. *Biochemistry* **40**: 4780–4791.

Fan L, Sanschagrin PC, Kaguni LS, Kuhn LA. 1999. The accessory subunit of mtDNA polymerase shares structural homology with aminoacyl-tRNA synthetases: implications for a

dual role as a primer recognition factor and processivity clamp. *Proc Natl Acad Sci USA* **96**: 9527–9532.

Felsenstein J. 1985. Confidence limits on phylogenies: an approach using the bootstrap. *Evolution* **39**: 783–791.

Felsenstein J. 2002. PHYLIP (Phylogeny Inference Package) version 3.6a. Distributed by the author **http://evolution.genetics.washington.edu/phylip.html**.

Foury F. 1989. Cloning and sequencing of the nuclear gene *MIP1* encoding the catalytic subunit of the yeast mitochondrial DNA polymerase. *J Biol Chem* **264**: 20552–20560.

Foury F, Roganti T, Lecrenier N, Purnelle B. 1998. The complete sequence of the mitochondrial genome of *Saccharomyces cerevisiae*. *FEBS Lett* **440**: 325–331.

Gietz RD, Triggs-Raine B, Robbins A, *et al*. 1997. Identification of proteins that interact with a protein of interest: applications of the yeast two-hybrid system. *Mol Cell Biochem* **172**: 67–79.

Gray H, Wong TW. 1992. Purification and identification of subunit structure of the human mitochondrial DNA polymerase. *J Biol Chem* **267**: 5835–5841.

Grimes GW, Mahler HR, Perlman PS. 1974. Letter: Mitochondrial morphology. *Science* **185**: 630–631.

Hazbun TR, Malmstrom L, Anderson S, *et al*. 2003. Assigning function to yeast proteins by integration of technologies. *Mol Cell* **12**: 1353–1365.

Heringa J. 1999. Two strategies for sequence comparison: profile-preprocessed and secondary structure-induced multiple alignment. *Comput Chem* **23**: 341–364.

Hobbs AE, Srinivasan M, McCaffery JM, Jensen RE. 2001. Mmm1p, a mitochondrial outer membrane protein, is connected to mitochondrial DNA (mtDNA) nucleoids and required for mtDNA stability. *J Cell Biol* **152**: 401–410.

Hu JP, Vanderstraeten S, Foury F. 1995. Isolation and characterization of ten mutator alleles of the mitochondrial DNA polymerase-encoding *MIP1* gene from *Saccharomyces cerevisiae*. *Gene* **160**: 105–110.

Insdorf NF, Bogenhagen DF. 1989. DNA polymerase gamma from *Xenopus laevis*. I. The identification of a high molecular weight catalytic subunit by a novel DNA polymerase photolabeling procedure. *J Biol Chem* **264**: 21491–21497.

Ito J, Braithwaite DK. 1990. Yeast mitochondrial DNA polymerase is related to the family A DNA polymerases. *Nucleic Acids Res* **18**: 6716.

Ito T, Tashiro K, Muta S, *et al*. 2000. Toward a protein-protein interaction map of the budding yeast: a comprehensive system to examine two-hybrid interactions in all possible combinations between the yeast proteins. *Proc Natl Acad Sci USA* **97**: 1143–1147.

Iyengar B, Luo N, Farr CL, *et al*. 2002. The accessory subunit of DNA polymerase gamma is essential for mitochondrial DNA maintenance and development in *Drosophila melanogaster*. *Proc Natl Acad Sci USA* **99**: 4483–4488.

Johnson AA, Tsai Y, Graves SW, Johnson KA. 2000. Human mitochondrial DNA polymerase holoenzyme: reconstitution and characterization. *Biochemistry* **39**: 1702–1708.

Kaguni LS. 2004. DNA polymerase gamma, the mitochondrial replicase. *Annu Rev Biochem* **73**: 293–320.

Kaufman BA, Newman SM, Hallberg RL, *et al*. 2000. In organello formaldehyde cross-linking of proteins to mtDNA: identification of bifunctional proteins. *Proc Natl Acad Sci USA* **97**: 7772–7777.

Kunkel TA, Roberts JD, Zakour RA. 1987. Rapid and efficient site-specific mutagenesis without phenotypic selection. *Methods Enzymol* **154**: 367–382.

Lecrenier N, Foury F. 2000. New features of mitochondrial DNA replication system in yeast and man. *Gene* **246**: 37–48.

Ling F, Shibata T. 2002. Recombination-dependent mtDNA partitioning: *in vivo* role of Mhr1p to promote pairing of homologous DNA. *EMBO J* **21**: 4730–4740.

Ling F, Shibata T. 2004. Mhr1p-dependent concatemeric mitochondrial DNA formation for generating yeast mitochondrial homoplasmic cells. *Mol Biol Cell* **15**: 310–322.

Luo N, Kaguni LS. 2005. Mutations in the spacer region of *Drosophila* mitochondrial DNA polymerase affect DNA binding, processivity, and the balance between Pol and Exo function. *J Biol Chem* **280**: 2491–2497.

MacAlpine DM, Perlman PS, Butow RA. 1998. The high mobility group protein Abf2p influences the level of yeast mitochondrial DNA recombination intermediates *in vivo*. *Proc Natl Acad Sci USA* **95**: 6739–6743.

Maleszka R, Skelly PJ, Clark-Walker GD. 1991. Rolling circle replication of DNA in yeast mitochondria. *EMBO J* **10**: 3923–3939.

Meeusen S, Nunnari J. 2003. Evidence for a two membrane-spanning autonomous mitochondrial DNA replisome. *J Cell Biol* **163**: 503–510.

Meeusen S, Tieu Q, Wong E, *et al*. 1999. Mgm101p is a novel component of the mitochondrial nucleoid that binds DNA and is required for the repair of oxidatively damaged mitochondrial DNA. *J Cell Biol* **145**: 291–304.

Miyakawa I, Sando N, Kawano S, *et al*. 1987. Isolation of morphologically intact mitochondrial nucleoids from the yeast *Saccharomyces cerevisiae*. *J Cell Sci* **88**: (4): 431–439.

Nicholas KB, Nicholas HBJ. 1997. GeneDoc: a tool for editing and annotating multiple sequence alignments. Distributed by the author **http://www.psc.edu/biomed/genedoc**.

Nunnari J, Marshall WF, Straight A, *et al*. 1997. Mitochondrial transmission during mating in *Saccharomyces cerevisiae* is determined by mitochondrial fusion and fission and the intramitochondrial segregation of mitochondrial DNA. *Mol Biol Cell* **8**: 1233–1242.

Ogur M, St. John R, Nagai S. 1957. Tetrazolium overlay technique for population studies of respiration deficiency in yeast. *Science* **125**: 928–929.

Olson MW, Wang Y, Elder RH, Kaguni LS. 1995. Subunit structure of mitochondrial DNA polymerase from *Drosophila* embryos. Physical and immunological studies. *J Biol Chem* **270**: 28932–28937.

Phadnis N, Ayres Sia E. 2004. Role of the putative structural protein Sed1p in mitochondrial genome maintenance. *J Mol Biol* **342**: 1115–1129.

Philippsen P, Stotz A, Scherf C. 1991. DNA of *Saccharomyces cerevisiae*. *Methods Enzymol* **194**: 169–182.

Sambrook J, Russell D. 2001. *Molecular Cloning: A Laboratory Manual*, 3rd edn. Cold Spring Harbor Laboratory Press: Cold Spring Harbor, NY.

Sheff MA, Thorn KS. 2004. Optimized cassettes for fluorescent protein tagging in *Saccharomyces cerevisiae*. *Yeast* **21**: 661–670.

Simossis VA, Heringa J. 2003. The PRALINE online server: optimising progressive multiple alignment on the web. *Comput Biol Chem* **27**: 511–519.

Steger HF, Sollner T, Kiebler M, *et al*. 1990. Import of ADP/ATP carrier into mitochondria: two receptors act in parallel. *J Cell Biol* **111**: 2353–2363.

Thompson JD, Gibson TJ, Plewniak F, *et al*. 1997. The CLUSTAL_X windows interface: flexible strategies for multiple sequence alignment aided by quality analysis tools. *Nucleic Acids Res* **25**: 4876–4882.

Uetz P, Giot L, Cagney G, *et al*. 2000. A comprehensive analysis of protein–protein interactions in *Saccharomyces cerevisiae*. *Nature* **403**: 623–627.

Vanderstraeten S, Van den Brule S, Hu J, Foury F. 1998. The role of 3′–5′ exonucleolytic proofreading and mismatch repair in yeast mitochondrial DNA error avoidance. *J Biol Chem* **273**: 23690–23697.

Williamson DH, Fennell DJ. 1979. Visualization of yeast mitochondrial DNA with the fluorescent stain 'DAPI'. *Methods Enzymol* **56**: 728–733.

Wong ED, Wagner JA, Gorsich SW, *et al*. 2000. The dynamin-related GTPase, Mgm1p, is an intermembrane space protein required for maintenance of fusion competent mitochondria. *J Cell Biol* **151**: 341–352.

Young M, Court D. 2004. Quick measurement of glucose concentration in *Saccharomyces cerevisiae* cultures. *Bull Genet Soc Can* **35**: 109–110.

Youngman MJ, Hobbs AE, Burgess SM, *et al*. 2004. Mmm2p, a mitochondrial outer membrane protein required for yeast mitochondrial shape and maintenance of mtDNA nucleoids. *J Cell Biol* **164**: 677–688.

Zelenaya-Troitskaya O, Newman SM, Okamoto K, *et al*. 1998. Functions of the high mobility group protein, Abf2p, in mitochondrial DNA segregation, recombination and copy number in *Saccharomyces cerevisiae*. *Genetics* **148**: 1763–1776.

Zelenaya-Troitskaya O, Perlman PS, Butow RA. 1995. An enzyme in yeast mitochondria that catalyzes a step in branched-chain amino acid biosynthesis also functions in mitochondrial DNA stability. *EMBO J* **14**: 3268–3276.